THE BELL SYSTEM TECHNICAL JOURNAL
Vol. 60, No. 9, November 1981
Printed in U.S.A.

High-Speed Measurement and Control of Fiber-Coating Concentricity

By D. H. SMITHGALL and R. E. FRAZEE

(Manuscript received May 19, 1981)

A technique has been implemented to measure and control the eccentricity of lightguide fiber in transparent polymer coating materials. It is based upon a model which describes the characteristics of a forward-scattered light pattern generated by transversely illuminating coated fiber with a laser beam. The model predicts the behavior of the principal characteristics of the pattern as a function of fiber eccentricity within the coating. The implementation automatically detects and controls the position of the dominant pattern feature to maintain an average fiber-coating concentricity within 2 μm over multikilometer lengths of fiber.

I. INTRODUCTION

The concentricity of an optical fiber in a plastic coating affects the fiber strength, transmission loss, and the connectorization process. Self-centering coating techniques, such as the flexible tip applicator,[1] or hydrodynamically designed applicators,[2] have not been completely effective in maintaining the fiber centered in the coating. An alternative to such passive fiber centering is to measure and control the location of the fiber in the coating.

Eichenbaum has described a technique in which the coated fiber is illuminated by a laser beam (Fig. 1) and the symmetry of certain features of the forward scattering pattern are used to determine coating concentricity.[3] His model analyzed coatings whose refractive index is greater than that of the fiber, and eccentricities are normal to the direction of the laser beam. The effects of refractive index and relative fiber and coating diameters for the concentric case are also described. The model is limited, however, to fiber offset normal to the direction of incidence and does not consider the effect of the fiber core upon the forward-scattered pattern.

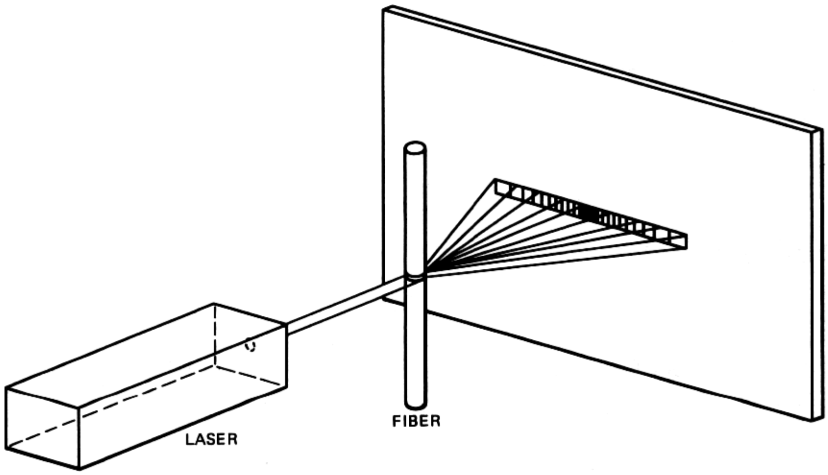

Fig. 1—Forward-scattering pattern generated from laser-illuminated fiber.

An alternate approach, first examined by Presby and subsequently described by Marcuse for silicone coatings, examines the backward-scattered pattern from a coated fiber illuminated by a laser beam.[4,5] The structure of the pattern is more complex than a forward-scattered pattern because the scattered light passes through the coated-fiber structure twice.

The technique of measuring fiber properties by forward-light scattering has been shown to be very powerful, and a similar approach could prove useful to automatically measure the fiber concentricity during the coating operation, and control the position of the fiber within the coating material.[6–9] Of the two scattering techniques described, the forward-scattering technique has the advantages that the pattern has a simpler structure, and as a practical matter, the forward-scattered pattern contains more light energy than the backward-scattered pattern, thus, requiring a smaller laser to provide sufficient information to a detector. In developing a centering control based upon forward-scattered light, the effects of both the fiber core and an arbitrary fiber eccentricity upon the structure of the scattering pattern must be considered.

II. CONCENTRIC FIBER RAY-SCATTERING MODEL

The smoothed envelope of the intensity of the forward-scattered pattern from a graded-index, multimode fiber coated with an epoxy acrylate material is shown in Fig. 2. The pattern is typical for fiber with a 50-μm core with 0.23 NA (numerical aperture), 125-μm clad

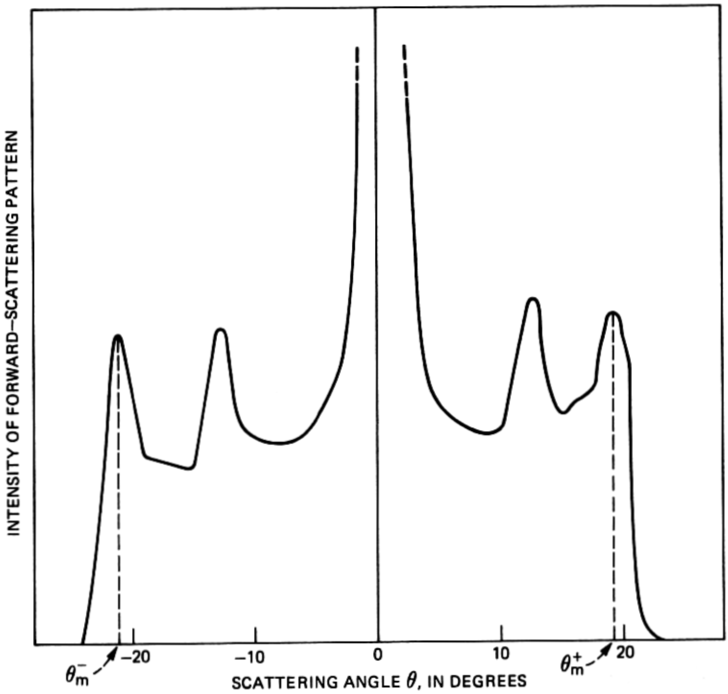

Fig. 2—Smoothed intensity of forward-scattered pattern for graded-index fiber in high-index coating.

diameter, and 250-μm coating diameter. The refractive indices of the cladding and coating are 1.457 and 1.539, respectively, at 0.6328 μm.

The structure of this pattern can be analyzed by considering the three-level concentric model shown in Fig. 3, where the radii are

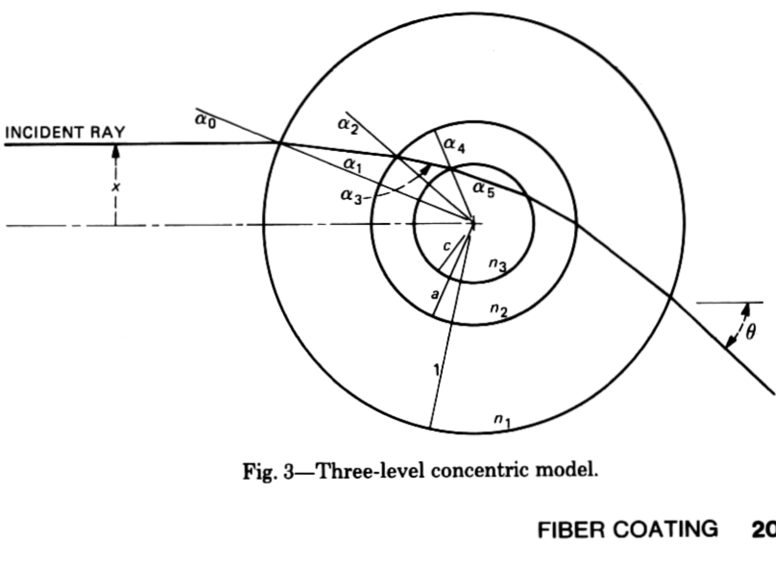

Fig. 3—Three-level concentric model.

normalized to the coating radius, and the refractive indices are assumed constant. The scattering angle θ for a ray striking the coating a distance x from the optical axis can be determined from the formula of Bouger,[10] when the ray passes through the core, as $x \leq n_2\, c$, and

$$\theta = 2\,(\alpha_0 - \alpha_1 + \alpha_2 - \alpha_3 + \alpha_4 - \alpha_5), \tag{1}$$

where

$$\begin{aligned} x &= \sin \alpha_0 \\ &= n_1 \sin \alpha_1 = n_1\, a \sin \alpha_2 \\ &= n_2\, a \sin \alpha_3 = n_2\, c \sin \alpha_4 \\ &= n_3\, c \sin \alpha_5. \end{aligned} \tag{2}$$

The exit angle, θ, for rays refracted through the cladding, $n_2\, c < x \leq n_1\, a$, is given by

$$\theta = 2\,(\alpha_0 - \alpha_1 + \alpha_2 - \alpha_3), \tag{3}$$

where the angles are defined in eq. (2).

In the case of a high-index coating, eq. (3) holds over the range $n_2\, c \leq x < n_2\, a$. In the range $n_2\, a \leq x < n_1\, a$, rays are reflected from the surface of the fiber, and the exit angle is given by

$$\theta = 2\,(\alpha_0 - \alpha_1 + \alpha_2 - \pi/2). \tag{4}$$

The exit angle for rays refracted through the coating only is

$$\theta = 2\,(\alpha_0 - \alpha_1). \tag{5}$$

For the parameters given above, the relationship between the scattering angle and the normalized incident ray position is shown in Fig. 4 for x between 0 and 1. For x in the range 0 to -1, $\theta(-x) = -\theta(x)$. Ray positions less than x_c pass through the core of the fiber; rays between x_c and x_2 pass through the fiber clad and coating. Ray positions greater than x_2 pass through the coating only.

Over the angular range θ_c to θ_u, there is an interference pattern generated by rays passing through both the core and cladding of the fiber. This interference is observed as an intensity maxima near ±10° in Fig. 2. The structure of the interference pattern depends upon the core index gradient,[11] and for typical near-parabolic index gradients, there exists a single intensity maximum whose location is nearer θ_c than θ_u. The angle θ_c is independent of core structure, but depends upon core diameter. For single-mode fibers, $\theta_c \to 0$, and there will be no measurable intensity peak in the scattered-light pattern corresponding to the core-clad interface.

The intensity maxima near ±20° in Fig. 2 result from the focusing

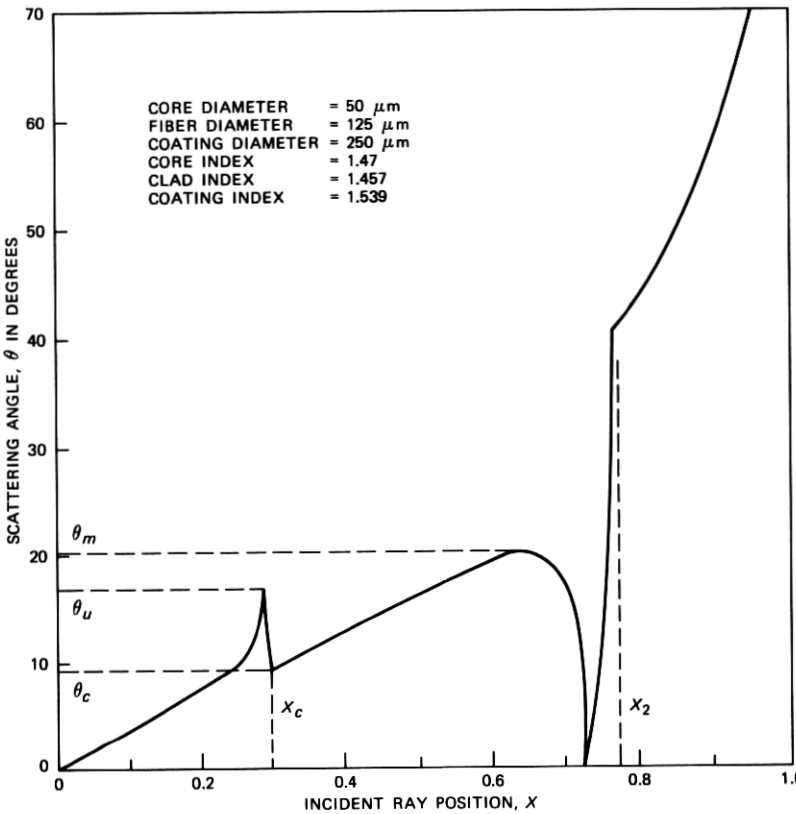

Fig. 4—Ray-scattering pattern for step-index, multimode fiber with high-index coating.

of rays passing near the clad-coating interface. The location of these caustics in Fig. 4 is the angle θ_m, where $d\theta/dx = 0$. If the slope of the inverse scattering curve $dx/d\theta$ is interpreted as the relative energy density of the scattered light, then $dx/d\theta \rightarrow \infty$ is a region of focused energy which will result in an intensity maximum. Conversely, the energy density of the forward-scattered pattern for angles greater than θ_m is very low. This is observed in Fig. 2 as an abrupt reduction in detected energy near the peak intensity at θ_m.

III. ECCENTRIC FIBER RAY-SCATTERING MODEL

The influence of fiber eccentricity within the coating upon the forward-scattered pattern may be determined by examining its effect upon the position of the intensity maximum at θ_m. The maxima at θ_c may or may not exist, depending upon the structure of the fiber. The results in the preceding section show that for typical single or multimode fibers, the effect of the core and the effect of the fiber/coating relationship upon the scattering pattern are distinct and separate. Therefore, in the subsequent development, a homogeneous fiber structure will be assumed with no loss of generality.

Consider the general nonconcentric structure of Fig. 5 in which the center of the fiber is displaced from the center of the coating by a distance d at an angle ϕ from incidence. The radii of the fiber and coating have been normalized to "a" and 1, respectively. The refractive indices are n_2 and n_1, respectively. Using Snell's Law and the geometric construction of Ref. 5, expressions for the angles describing the ray path can be determined by modifying the equations describing backscattered rays to describe the refraction of forward-scattered rays.

$$\alpha_0 = \sin^{-1} x. \tag{6}$$

$$\alpha_1 = \sin^{-1}\left(\frac{1}{n_1}\sin\alpha_0\right). \tag{7}$$

$$\gamma_1 = \frac{1}{a}\sin\alpha_1 - \frac{d}{a}\sin(\alpha_0 - \alpha_1 + \phi). \tag{8}$$

$$\alpha_2 = \sin^{-1}\gamma_1. \tag{9}$$

$$\gamma_2 = \frac{n_1}{n_2}\sin\alpha_2. \tag{10}$$

$$\alpha_3 = \sin^{-1}\gamma_2. \tag{11}$$

$$\alpha_4 = \alpha_3. \tag{12}$$

$$\alpha_5 = \alpha_2. \tag{13}$$

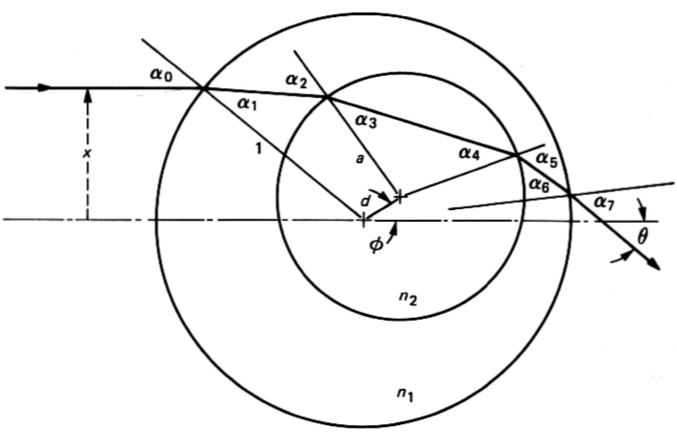

Fig. 5—Refracted ray in two-level structure with offset core.

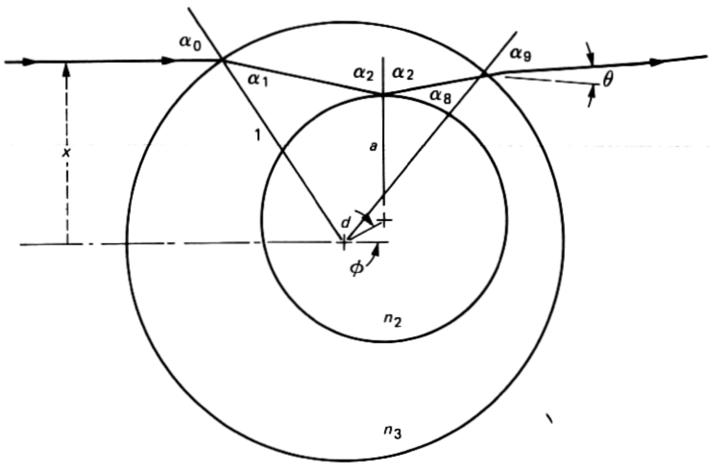

Fig. 6—Internal reflected ray in two-level structure with offset core.

$$\alpha_6 = \sin^{-1}\{a \sin \alpha_2 + d \sin[\alpha_0 - \alpha_1 + 2(\alpha_2 - \alpha_3) + \phi]\}. \tag{14}$$

$$\alpha_7 = \sin^{-1}(n_1 \sin \alpha_6). \tag{15}$$

These equations represent an arbitrary ray passing through the coated fiber. Certain conditions, however, yield internally reflected rays or rays passing only through the coating material. Hence, special cases of eqs. (6) to (15) need to be considered in determining the exit angle $\theta(x)$.

For a ray which passes through the fiber and coating,

$$\gamma_1, \gamma_2 < 1, \quad \text{and} \tag{16}$$

$$\theta = (\alpha_0 - \alpha_1) + 2(\alpha_2 - \alpha_3) + (\alpha_7 - \alpha_6). \tag{17}$$

For a ray which passes through the coating only,

$$\gamma_1 > 1, \quad \text{and} \tag{18}$$

$$\theta = 2(\alpha_0 - \alpha_1). \tag{19}$$

For a ray which passes through the coating and is reflected from the fiber surface (Fig. 6),

$$\gamma_1 < 1.$$

$$\gamma_2 > 1. \tag{20}$$

$$\gamma_3 = \alpha_0 - \alpha_1 + \phi + 2\alpha_2 - \pi/2. \tag{21}$$

$$\alpha_8 = \sin^{-1}(a \sin \alpha_2 + d \sin \gamma_3). \tag{22}$$

$$\alpha_9 = \sin^{-1}(n_1 \sin \alpha_8). \tag{23}$$

$$\theta = \alpha_0 + 2\alpha_2 + \alpha_9 - \alpha_1 - \alpha_8 - \pi. \tag{24}$$

There is one additional case occurring when $n_1 \sin \alpha_6 > 1$ or $n_1 \sin \alpha_8 > 1$, which represents total internal reflection at the point where the ray should exit the coating.

Equations (6) to (24) can be used to generate ray-scattering angles $\theta(x)$. By appropriate choices of d and ϕ, scattering angles for arbitrary fiber eccentricity may be examined.

IV. RESULTS FOR TWO-LEVEL MODEL

For the purpose of investigating the effect of fiber eccentricity, consider the model wherein the ratio of core and outer diameter $a = 0.5$, and the refractive indices of the core and outer layers are 1.457 and 1.539, respectively. These index values correspond to those of fused silica and an epoxy acrylate coating material. The effects of changing the material indices or the fiber/coating diameter ratio were examined in Ref. 3 for a concentric structure.

The effect of offset "d" along the direction of incidence ($\phi = 0$), and normal to the direction of incidence ($\phi = \pi/2$*) upon θ_m is shown in Fig. 7. For each case, there is a θ_m corresponding to refraction of the light rays to both sides of the axis of the incident light. The angle θ_m^+ results from incident rays striking the fiber at normalized positions in the range 0 to +1, and the angle θ_m^- results from incident rays striking the fiber for x between 0 and −1. There is a symmetry such that θ_m^+ and θ_m^- exchange roles for $\phi = \phi + \pi$. This is illustrated in Fig. 7 by showing the dependence of θ_m upon negative d.

For the case $\phi = 0$, the loci of θ_m^+ and θ_m^- are symmetric about the vertical axis with increasing separation as the fiber is displaced away from the laser source. For d varying from −0.2 ($d = 0.2$ @ $\phi = \pi$) to $d = 0.2$, θ_m varies from 18 to 26 degrees.

For the case $\phi = \pi/2$, the maxima θ_m^+ and θ_m^- are symmetric about the axis only for $d = 0$. For increasing d at $\phi = \pi/2$, θ_m^+ increases and θ_m^- decreases. Furthermore, the separation increases as d increases, from 41 degrees at $d = 0$ to 54 degrees at $d = 0.2$. For $\phi = 3\pi/2$, the roles of θ_m^+ and θ_m^- are reversed.

At a fiber displacement of approximately $d = 0.2$, the ray generating θ_m^+ is totally internally reflected at the point where it would exit the coating material, and the scattering-pattern feature corresponding to θ_m^+ does not exist.

For the more general case of an arbitrary ϕ, define the separation of

* In the subsequent discussion, the angle of the fiber offset is given in radians and the ray-scattering angle is given in degrees.

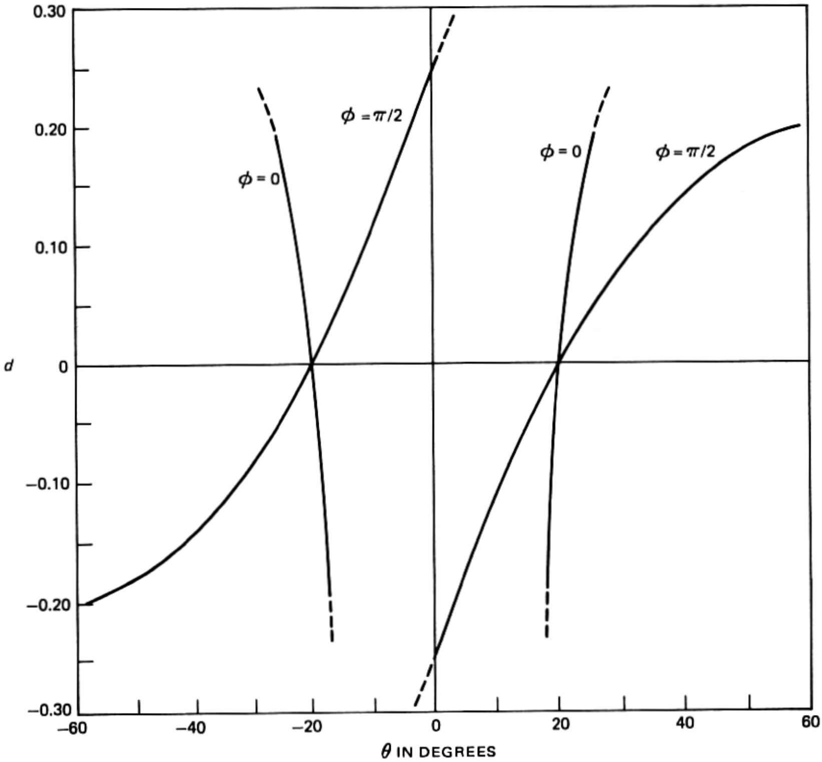

Fig. 7—Locus of intensity maxima θ_m as a function of spatial offset for two angles of offset.

the scattering-pattern intensity maxima as

$$\Delta = \theta_m^+ - \theta_m^-. \tag{25}$$

It has been illustrated in the previous discussion that Δ as a function of both d and ϕ will provide an indication of the composite behavior of the scattering pattern. In addition, Δ is a factor in the measured eccentricity.

$$E = \frac{\theta_m^+ + \theta_m^-}{\Delta}. \tag{26}$$

Figure 8 shows a plot of Δ as a function of the offset orientation, ϕ, with the offset magnitude, d, as a parameter. The pattern is cyclic in ϕ as expected. For $d > 0.15$, $\Delta \rightarrow \infty$ near the orientation $\phi = \pm\pi/4$. The intensity maxima θ_m^+ does not exist for $d > 0.15$ at this angular orientation. The fiber is sufficiently close to the surface of the coating that the cumulative refraction of the light rays remains monotonic with ray height, x, as in the case of the homogeneous medium.

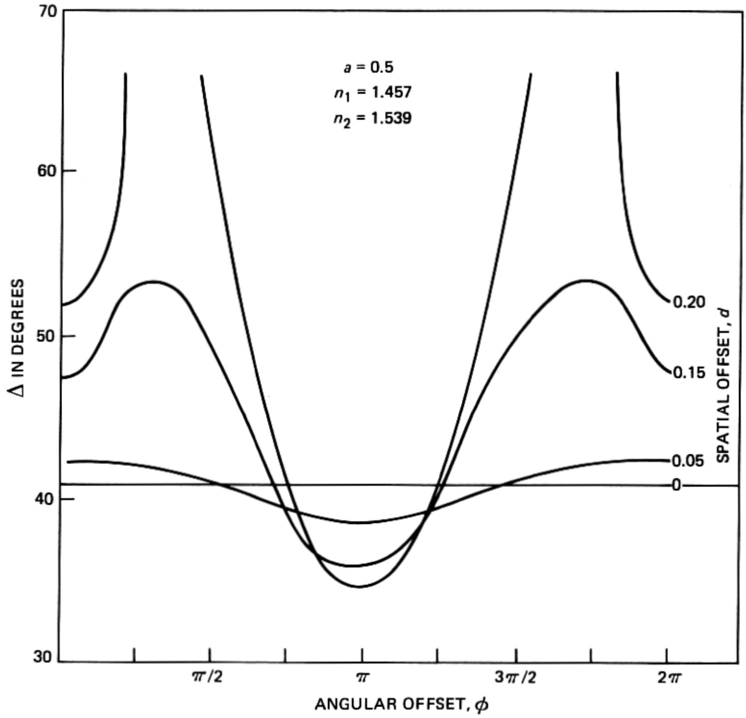

Fig. 8—Separation (Δ) of intensity maxima as a function of spatial and angular offset with respect to incident laser beam.

Therefore, there is no region in which scattered energy is concentrated for eccentricities greater than 15 percent of the coating radius. This condition limits the range over which a high-intensity feature could be used to detect fiber eccentricity. Subsequently, it will be shown that this is a minor restriction.

V. OPTICAL DESIGN FOR COATING CONCENTRICITY MONITOR

The model developed in Section III has shown that if the intensity maxima at θ_m^+ and θ_m^-, or, correspondingly, the abrupt change in intensity at the edges of the pattern, could be detected, their position would provide a monotonic measure of the eccentricity of the fiber within the coating. By illuminating the coated fiber in two orthogonal directions, the degree of fiber eccentricity is uniquely established. The fiber may be centered within the coating by establishing symmetry within each of the two orthogonal patterns.

The optical layout for the automatic detection system is shown in Fig. 9. The beam for a 1-mW HeNe laser is attenuated by a neutral density filter and split into two equal-intensity beams which are each

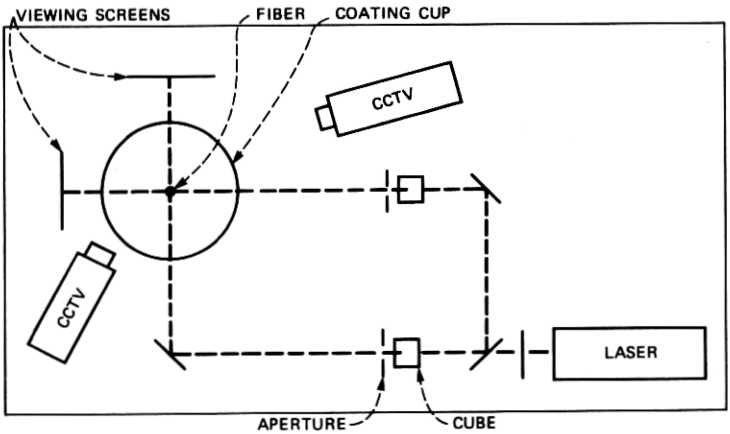

Fig. 9—Optics layout for automatic centering unit.

reflected to intersect at the fiber. Located approximately four centimeters behind the fiber is a viewing screen of white bond paper. The paper provides a high contrast background, and partially diffuses the scattering pattern, eliminating the fine structure corresponding to interference of refracted and reflected rays. The scattering pattern, as viewed on the screen, appears as a bright bar on either side of the very bright central spot (Fig. 10). At the end of each bar is a spot of slightly greater intensity corresponding to the outer peaks of Fig. 2. For multimode fiber, a second bright spot may be discerned between the central peak and the edge of the bright region.

The scattering pattern is viewed by a closed circuit television (CCTV) camera through a 0.633-μm interference filter. The filter permits the device to operate in normal room lighting conditions, while only the scattering pattern is observed. The camera is mounted such that the scattering pattern is crossed by a multiplicity of scan lines. Thus, along each scan line the intensity of the pattern is sampled once. By extracting this information from the CCTV output, the scattering pattern can

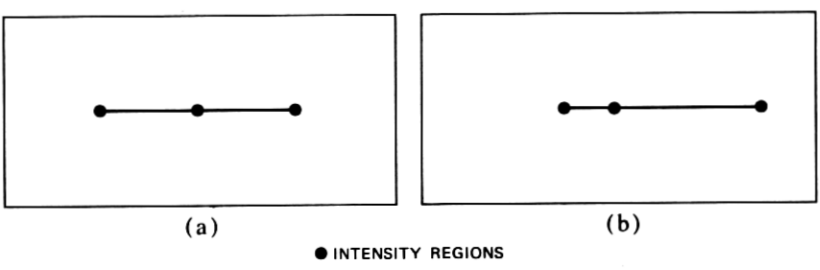

Fig. 10—Forward-scattering patterns as seen on viewing screen. (a) Fiber centered in coating. (b) Fiber eccentric in coating.

be reconstructed as in Fig. 2. Furthermore, the location of important features within the pattern can be determined by counting the number of samples, or scan lines, between features. With the full-field view of CCTV, the detector is insensitive to tilt in the scattering pattern resulting from an angularly-misaligned camera or fiber.

To determine the centered position of the fiber within the coating, the forward-light-scattered pattern is made symmetric with respect to a central intensity maximum of the pattern, generated by the incident laser beam. If the coated fiber is not centered in the beam, a slight offset in the pattern with respect to the central peak exists, and when corrected by moving the coating applicator, results in an off-center coating. In addition, centering the coated fiber in the laser beam maximizes the energy transferred from the beam into the scattering pattern, and ensures that the two wings of the scattering pattern will have equal energy, maximizing the sensitivity of the measurement system.

To align the laser beams to the coated fiber, a rotatable cube, mounted on the shaft of a small servo motor is located in each optical path. An aperture placed between the cube and the viewing screen eliminates spurious scattering effects from the corners of the cube.

The optical components, screens, and CCTVs are mounted on a platform with the coating cup. The platform is adjustable with respect to a fixed base plate which, in turn, is attached to the fiber draw tower. Thus, the coated fiber structure is fixed with respect to the illuminating laser beams, and the fiber moves within the coating, limited by the orifice in the tip of the applicator.

VI. VIDEO SIGNAL PROCESSING

Two CCTV cameras are mounted such that each views one of the orthogonally mounted viewing screens and cuts the projected forward-scattering pattern with a plurality of horizontal scan lines. The camera outputs are treated independently of each other but via identical circuitry (Fig. 11). For each, the composite video signal is separated into the video and synchronization components.

The video portion of the signal is input to two separate integrator circuits. One integrator sums the collective value of all the video pulses contained in one complete vertical field. Therefore, the output voltage is proportional to the total energy contained in the forward-scattered pattern. This signal, input to the microprocessor through an analog-to-digital (A/D) converter, is used to center the laser beam on the coated fiber. The update rate of the signal strength measurement is equal to the vertical field scan rate (60 Hz).

The second integrator sums the signal levels contained in each horizontal scan line. The output, controlled by line synchronization

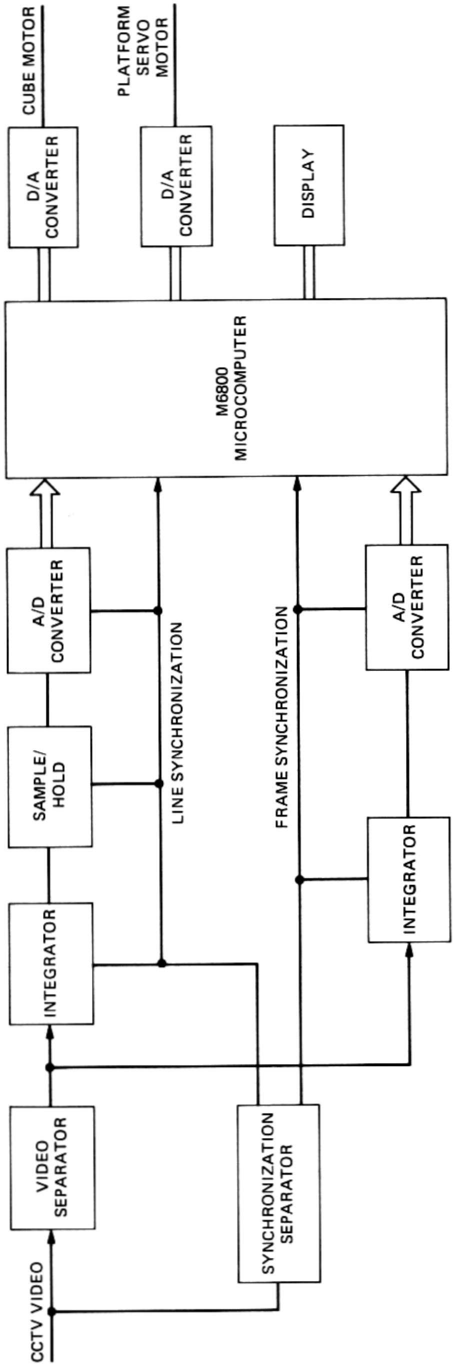

Fig. 11—Video signal processing circuit.

pulses to form a serialized boxcar representation of the envelope, is input to a high-speed A/D converter which converts each scan line level to eight bits of binary data, which are input to the microprocessor. The video scan line signal is conditioned at the horizontal scan rate of approximately 63 μs.

VII. MEASURE OF FIBER ECCENTRICITY

Once the laser beam has been centered on the coated fiber structure the envelope of the scattering pattern is examined to determine fiber eccentricity. Establishing a reference on the frame synchronization pulse, and subsequently, on each of the line synchronization pulses, 230 consecutive samples are read from the A/D converter. Each sample represents the intensity of the scattering pattern detected during line scan.

The data is scanned to locate the intensity changes which correspond to the edges of the laser beam and the forward-scattered pattern. From the scattering model it is known that an intensity maximum must occur near the locations at which the intensity goes to zero.

Let $\{X_i,\ i = 1, \cdots, n\}$ be the intensities of the samples $\{i\}$. A maxima is defined as:

$$M_i\colon X_i - X_{i+1} \geq 0$$
$$X_i - X_{i-1} > 0. \tag{27}$$

The two maxima corresponding the θ_m^+ and θ_m^- may be determined by searching the data near the locations of the edges of the pattern. From the relative locations of the central intensity maximum corresponding to the laser beam and the two maxima, the angles θ_m^+ and θ_m^- can be determined and the eccentricity measure

$$e = \theta_m^+ + \theta_m^- \tag{28}$$

defined. Equation (28) represents a monotonic measure of fiber eccentricity, since it can take on both positive and negative values. Furthermore, the function can be used directly to generate a corrective control signal to center the fiber in the coating.

VIII. CONTROL OF FIBER POSITION

The coating material, with a viscosity of ~50 poise at room temperature, presents a strong dampening effect on the motion of the fiber. Consequently, when the cut is moved with respect to the fiber, a settling time of several seconds is observed. Conversely, once the fiber is centered within the coating cup it will tend to remain centered such that readjustment is only occasionally required. It has been observed that fifteen minutes may be required to reach this equilibrium state, with frequent position adjustments necessary prior to reaching equilibrium.

The algorithm implemented for fiber positioning is a deadband control, where for e given by eq. (28), the control u is:

$$
\begin{aligned}
u &= 0 \qquad && 1 \le e \le 1 \\
u &= u_0 \qquad && e > 1 \\
u &= -u_0 \qquad && e < -1.
\end{aligned}
\tag{29}
$$

The value of u_0 is selected large enough to overcome friction and hysteresis in the servo motors and platform transport mechanism, yet, small enough to account for the slow dynamic response of the fiber moving through the coating material. The deadband about the point of pattern symmetry prevents the servo motor from constantly responding to small disturbances resulting from short-term fluctuations in eccentricity, or single quantum steps in the computation of the eccentricity function [eq. (25)]. The normal system condition for a process in equilibrium is one of quiescence.

For the typical case of an epoxy acrylate-coated silica fiber, with 125-μm-fiber diameter and 250-μm-outer diameter, a scattering pattern with the intensity maxima at ± 20 degree is generated. A pattern nearly 4 cm wide projected onto the viewing screen is intersected by approximately 60 horizontal scan lines on the CCTV. With the algorithm previously described, centering is controlled within ± 1 part in 30, or $\pm 2/3$ degree. From Fig. 7, the sensitivity to fiber offset normal to the incident laser beam is 1 percent of the coating radius per degree shift in concentricity. Therefore, the control of the average concentricity is ± 1 μm.

Localized fluctuations may exceed this value. Experience has shown that long lengths of fiber may be coated with coating concentricities within 1.5 percent of the coating diameter.

IX. CONCLUSION

A multilevel model for a lightguide fiber coated with material with refractive index greater than that of the fiber, has been used to determine characteristics of the forward-scattered pattern with respect to the coating concentricity. The results of the model have been used as a basis for a system which detects and controls the average position of the fiber in the coating within 2 μm. Experimentally, the fiber-coating concentricity has been maintained within 1.5 percent over multikilometer lengths of fiber. With this control, the predicted limitation in detectable eccentricity of 7.5 percent of coating diameter is not a significant factor.

REFERENCES

1. A. C. Hart and R. V. Albarino, "An Improved Fabrication Technique For Applying Coatings to Optical Fiber Waveguides," Technical Digest of Topical Meeting on Optical Fiber Transmission II, Williamsburg, Virginia, February 22–4, 1977, Paper TuB2.
2. P. W. France, P. L. Dunn, and M. H. Reeve, "Plastic Coating of Glass Fibers and Its Influence on Strength," Fiber and Integrated Optics, *2,* No. 3–4, pp. 267–86.
3. B. R. Eichenbaum, "The Centering of Optical Fiber Coatings by Monitoring Forward Scattering Patterns—Theory and Practice," B.S.T.J., *59,* No. 3 (March 1980), pp. 313–32.
4. H. M. Presby, "Geometrical Uniformity of Plastic Coatings on Optical Fibers," B.S.T.J., *55,* No. 10 (December 1976), pp. 1525–37.
5. D. Marcuse and H. M. Presby, "Optical Fiber Coating Concentricity: Measurement and Analysis," Appl. Optics, *16,* No. 9 (September 1977), pp. 2383–90.
6. D. H. Smithgall, L. S. Watkins, and R. E. Frazee, "High Speed Non-contact Fiber Diameter Measurement Using Forward Light Scattering," Appl. Optics, *16,* No. 9 (September 1977), pp. 2395–402.
7. L. S. Watkins, "Scattering From Side—Illuminated Clad Glass Fibers for Determination of Fiber Parameters," J. Opt. Soc. of Am., *64* (June 1974), pp. 767–72.
8. M. A. G. Abushagur and N. George, "Measurement of Optical Fiber Diameter Using Fast Fourier Transform," Appl. Opt., *19,* No. 12 (June 15, 1980), pp. 2031–3.
9. L. S. Watkins and R. E. Frazee, "High Speed Measurement of Core Diameter of a Step Index Optical Fiber," Appl. Opt., *19,* No. 22 (November 15, 1980), pp. 3756–62.
10. M. Born and E. Wolf, *Principles of Optics*, New York: Pergamon Press, 1964.
11. L. S. Watkins, "Laser Beam Refraction Traversely Through a Graded Index Preform to Determine Refractive Index Ratio and Gradient Profile," Appl. Opt., *18,* No. 13 (July 1, 1979), pp. 2214–22.